Stepwise Neoplastic Transformation of a Telomerase Immortalized Fibroblast Cell Line

Samantha Zongaro,[1] Elisa de Stanchina,[2] Tina Colombo,[3] Maurizio D'Incalci,[3] Elena Giulotto,[4] and Chiara Mondello[1]

[1]Istituto di Genetica Molecolare, Consiglio Nazionale della Ricerche, Pavia, Italy; [2]Dipartimento di Genetica e Microbiologia "Adriano Buzzati Traverso," University of Pavia, Pavia, Italy; [3]Cold Spring Harbor Laboratory, Cold Spring Harbor, New York; and [4]Istituto di Ricerche Farmacologiche "Mario Negri," Milan, Italy

Abstract

We have described recently a human fibroblast cell line immortalized through ectopic telomerase expression (cen3-tel), in which the extension of the life span was associated with the appearance of chromosomal aberrations and with the ability to grow in the absence of solid support. As reported in this article, on further propagation in culture, cen3tel cells became neoplastically transformed, being able to form tumors in nude mice. The analysis of the cells, during the gradual transition toward the tumorigenic phenotype, allowed us to trace cellular and molecular changes associated with different phases of transformation. At the stage in which they were able to grow in agar, cen3tel cells had lost contact growth inhibition but still retained the requirement of serum to proliferate and were not tumorigenic in immunocompromised mice. Moreover, they showed a down-regulation of the *INK4A* locus and were resistant to oncogenic Ras-induced senescence but still retained a functional p53. Subsequently, cen3tel cells became tumorigenic, lost p53 function because of a mutation in the DNA-binding motif, and overexpressed c-*myc*. Interestingly, tumorigenic cells did not carry activating mutations either in the *ras* proto-oncogenes (H-*ras*, N-*ras*, and K-*ras*) or in B-*raf*. Cen3tel cells gradually became hyperdiploid but did not display centrosome abnormalities. To our knowledge, cen3tel is the first telomerase immortalized fibroblast line, which became neoplastically transformed. In this system, we could associate a down-regulation of the *INK4A* locus with anchorage-independent growth and with resistance to Ras-induced senescence and link *p53* mutations and c-*myc* overexpression with tumorigenicity. (Cancer Res 2005; 65(24): 11411-8)

Introduction

Cellular transformation is a stepwise process, and several successive genetic or epigenetic changes are required for the development of a neoplastic phenotype. A typical feature of neoplastic cells is the ability to divide indefinitely (1). In human cells, an indefinite replicative potential is strictly related to the capability to maintain telomeres, the terminal parts of the chromosomes (2).

Telomeres are DNA-protein structures essential for the maintenance of chromosome stability (3); they are elongated by the specialized enzyme telomerase, a reverse transcriptase ribonucleoprotein, which adds telomeric repeats to the 3′ end of the telomeric strand, by copying the template sequence present in its RNA moiety (4). In most normal somatic cells, telomerase activity is too low to elongate telomeres (5), which thus shorten at each cell division (6).

Compelling evidence has been obtained showing that telomere shortening is an important mechanism limiting the life span of normal human somatic cells in culture (7, 8). When one or a few telomeres shorten below a threshold level, cells arrest in the cell cycle, entering a phase known as cellular senescence, probably because short telomeres are sensed as DNA double-strand breaks and activate DNA damage checkpoints (9, 10). The *p53* tumor suppressor gene plays a major role in triggering the cellular response to short telomeres, transactivating the $p21^{CIP1}$ gene, which codes for a cyclin-dependent kinase (cdk) inhibitor. The pRB tumor suppressor pathway is also involved in cellular senescence; in fact, it has been shown that senescence can be bypassed when the p53 and/or pRB functions are inactivated using different strategies (11–13).

Within the pRB pathway, the $p16^{INK4A}$ gene takes an important part in cellular senescence (14–17). This gene is up-regulated in replicative arrested cells; the signals triggering $p16^{INK4A}$ expression during senescence are presently unknown, and the possible role of telomere dysfunction in its induction is controversial (18, 19). $p16^{INK4A}$ interacts with the cdk4 and cdk6, preventing pRB phosphorylation (20). In the absence of phosphorylation, pRB does not release the E2F transcription factor, hampering the activation of genes involved in cell cycle progression and thus leading to replicative arrest. Given its role in cell cycle control, $p16^{INK4A}$ plays also an important role in tumor suppression; in fact, loss of its expression is frequently observed in cancer cells (21). $p16^{INK4A}$ is encoded by the *INK4A* locus, which contains also the $p14^{ARF}$ gene. $p16^{INK4A}$ and $p14^{ARF}$ partially overlap, sharing the second and third exons, but are transcribed using different reading frames. $p14^{ARF}$ functionally intersects with p53 (22) and inhibits growth of primary cells through the p53 pathway, but its possible role in tumorigenesis is still elusive (23).

The link between telomere maintenance and unlimited proliferative potential was experimentally shown by introducing the gene coding for the human telomerase catalytic subunit (*hTERT*) under the control of a constitutive promoter into normal human somatic cells. Expression of the catalytic subunit leads to the reconstitution of telomerase activity and allows cells to abrogate cellular senescence and to divide indefinitely (8). Early studies indicated that telomerase-based immortalization of somatic cells was not associated with the acquisition of features typical of transformation (24).

Note: Supplementary data for this article are available at Cancer Research Online (http://cancerres.aacrjournals.org/).

Requests for reprints: Chiara Mondello, Istituto di Genetica Molecolare, CNR, Via Abbiategrasso 207, 27100 Pavia, Italy. Phone: 39-0382-546332; Fax: 39-0382-422286; E-mail: mondello@igm.cnr.it.

doi:10.1158/0008-5472.CAN-05-1140

More recently, we showed that telomerase immortalized fibroblasts can actually acquire a transformed phenotype. We introduced the *hTERT* cDNA into a fibroblast strain derived from a centenarian individual and isolated an immortalized cell line (cen3tel). During culture propagation, cen3tel cells displayed typical characteristics of transformed cells (25), such as chromosomal instability and the ability to grow in the absence of solid support. At the stage in which they were able to grow in agar, cen3tel cells were not tumorigenic in nude mice, indicating that they were not neoplastically transformed (25).

In the work presented here, we studied the further evolution of this *hTERT* immortalized cell line, repeated the inoculation of cen3tel cells into nude mice at later culture passages, and found that they had become tumorigenic. In addition, we investigated genomic changes possibly related to transformation. In particular, in cen3tel cells at different stages of culture propagation, we analyzed the karyotype, centrosome number, contact inhibition, and serum requirement to grow. We monitored the status of the *p53* tumor suppressor gene and the *ras* proto-oncogenes together with the level of expression of the *INK4A* locus and c-*myc* and $p21^{CIP1}$ genes and the response to overexpression of an activated *ras* oncogene.

Materials and Methods

Cell cultures. The telomerase immortalized cell line cen3tel was obtained from primary cen3 fibroblasts, derived from a centenarian individual, by infection with an *hTERT*-containing retrovirus as described in ref. 25. Primary and immortalized cells were grown in DMEM supplemented with 10% fetal bovine serum (BioWhittaker, Walkersville, ME), 2 mmol/L glutamine, and 1% nonessential amino acids (Euroclone, Pero (Mi), Italy). The ability to grow in the absence of solid support, tumorigenicity in nude mice, and karyotype were analyzed as described in Mondello et al. (25).

Indirect immunofluorescence. Cells (10^5) were seeded on a coverslip in a 3-cm Petri dish and incubated at 37°C for 24 hours. To detect p53 induction, cells were UV irradiated with 20 J/m^2 using a Philips TUV lamp (15 W; Philips, Eindhoven, the Netherlands). After 24 hours, cells were fixed for 7 minutes with 2% cold paraformaldehyde in PBS and treated for 7 minutes with 0.5% Triton in PBS. Cells were then incubated for 1 hour at 37°C with the primary anti-p53 antibody DO-1 (Santa Cruz Biotechnology, Santa Cruz, CA) diluted 1:50. Antibody binding was revealed with a rhodamine-labeled secondary antibody. To detect centrosomes and spindle fibers, cells were fixed for 5 minutes with ice-cold acetone and for 5 additional minutes with ice-cold methanol. Cells were then treated with 0.01% Triton in PBS. After a 30-minute blocking step with 0.1% bovine serum albumin in PBS, cells were incubated overnight at 4°C with the antibodies against γ-tubulin [rabbit polyclonal affinity-purified antibody (Sigma-Adrich, St. Louis, MO), diluted 1:150, for double staining of centrosomes and fibers and clone GTU-88 (Sigma-Adrich,), diluted 1:300, for single centrosome staining] and against α-tubulin [clone DM1A (Sigma-Adrich) diluted 1:500]. The bindings of the two antibodies were revealed with a rhodamine-labeled secondary antibody and a Cy2-labeled secondary antibody, respectively. To detect S-phase cells, 5×10^4 cells were seeded in 3-cm Petri dish with either 10% or 0.5% fetal bovine serum and after 1 and 6 days were incubated in the presence of 12 μg/mL bromodeoxyuridine for 30 minutes at 37°C. Cells were fixed on ice with 70% ethanol for 30 minutes, treated with 2 N HCl for 20 minutes, and then incubated with 0.1 mol/L sodium tetraborate (pH 8.5) for 5 minutes. Incubation with the anti-bromodeoxyuridine antibody (Becton Dickinson, Franklin Lakes, NJ) diluted 1:20 was carried out for 1 hour at 37°C. Antibody binding was revealed with a Cy2-labeled secondary antibody. Slides were analyzed with the Olympus microscope IX71, and images were taken with the digital camera Camedia 4000 (Olympus, Shinjuku-ku, Tokyo, Japan).

RNA extraction, Northern blot, and reverse transcription-PCR. Total RNA was extracted from actively dividing cells using the Trizol reagent (Invitrogen, Carlsbad, CA). Total RNA (15 μg) of each sample was separated on formaldehyde denaturing agarose gels (1.5%) and transferred onto nylon membranes (Zetaprobe GT, Bio-Rad Laboratories, Hercules, CA). Membranes were probed either with a DNA fragment comprising the coding region of the $p16^{INK4A}$ cDNA or with a probe for the third exon of c-*myc*. Final washings were done in 0.2× SSC and 0.5% SDS at 65°C for 1 hour. Each membrane was reprobed with a DNA fragment covering the *β-actin* cDNA.

For reverse transcription-PCR (RT-PCR), total RNA (2 μg) was reverse transcribed with the Moloney murine leukemia virus reverse transcriptase (Promega, Madison, WI) in the presence of 0.5 μg oligo(dT) (Promega) and 200 units enzyme in a final volume of 25 μL. cDNA (2 μL each) was PCR amplified using 2 units Taq DNA polymerase (Promega). The following primers and annealing temperature were used: $p16^{INK4A}$ forward 5′-GAGCAGCATGGAGCCTTCGG and reverse 5′-CATGGTTACTGCCTC-TGGTG (62°C), $p14^{ARF}$ forward 5′-AGGGTTTTCGTGGTTCACAT and reverse 5′-CTGCCCATCATCATGACCT (64°C), and *glyceraldehyde-3-phosphate dehydrogenase* (*GAPDH*) forward 5′-TCCACCACCCTGTTGCTGTA and reverse 5′-ACCACAGTCCATGCCATCAC (60°C). For each pair of primers, PCR was carried out for 30 cycles.

Mutation analysis of *p53*, H-*ras*, N-*ras*, K-*ras*, and B-*raf*. Mutations in the *p53* gene were searched in cDNA samples prepared from the different cell lines. Total RNA (2 μg) was reversed transcribed as described above and cDNA (5 μL) was amplified using the GeneAmp XL PCR kit (Applera, Norwalk, CT) according to the manufacturer's instruction. PCR was carried out for 35 cycles with an annealing temperature of 68°C and with the following primers: forward 5′-CCATGGAGGAGCCGCAGTCAGATCC and reverse 5′-GAAGTGGAGAATGTCAGTCTGAGTCAGGCC. The amplified fragment, which spans the entire p53 cDNA, was purified from gel and cloned using the pGEM-T Easy Vector System (Promega). DNA was extracted from single bacterial colonies and sequenced using the Big Dye terminator version 3.1 by the Biomolecular Research Center of the University of Padova (Padova, Italy).

Search for mutations at codons 12/13 and 61 of the *ras* genes was done by direct sequencing of genomic PCR products. The following primers were used: forward 5′-GCTGTGGGTTTGCCCTTCAGA and reverse 5′-TATCCTG-GCTGTGTCCTGGGC (H-*ras* codon 12/13), forward 5′-GGGAGTCCCT-CGTCTCAGCAC and reverse 5′-CACGGGGTTCACCTGTACTGGT (H-*ras* codon 61), forward 5′-AGGATGGGGGTTGCTAGAAAACT and reverse 5′-CGACAAGTGAGAGACAGGATCAGGT-3′ (N-*ras* codon 12/13), forward 5′-CAGATAGGCAGAAATGGGCTTGA and reverse 5′-CCTCATTTCCCCA-TAAAGATTCAGA (N-*ras* codon 61), forward 5′-GGTGAGTTTGTAT-TAAAAGGTACTG and reverse 5′-TGAAAATGGTCAGAGAAACCT (K-*ras* codon 12/13), and forward 5′-AATGTCTTTTCAAGTCCTTTGCC and reverse 5′-GCATGGCATTAGCAAAGACTCAAA-3′ (K-*ras* codon 61). Mutations in exons 11 and 15 of the B-*raf* genes were searched by denaturing gradient gel electrophoresis analysis as described in ref. 26.

Western blot analysis. To prepare whole-cell lysates for Western blot analysis, cells were lysed in coimmunoprecipitation buffer [0.5% NP40, 10 mmol/L Tris-HCl (pH 7.6), 140 mmol/L NaCl, 5 mmol/L EDTA (pH 8.0)] followed by addition of protease inhibitor cocktail (Sigma-Aldrich) and 2 mmol/L $NaVO_4$. For each sample, proteins (50 μg) were loaded on the gels. Western blot analysis was done using the following antibodies: anti-$p16^{INK4A}$ antibody (C20, Santa Cruz Biotechnology) diluted 1:200, anti-c-myc antibody (Ab-1, Oncogene, San Diego, CA) diluted 1:500, anti-$p21^{CIP1}$ antibody (C-19, Santa Cruz Biotechnology) diluted 1:200, anti-p53 antibody DO-1 diluted 1:200, and anti-γ-tubulin antibody (clone GTU-88) diluted 1:15,000. All primary antibodies were probed by a secondary horseradish peroxidase–conjugated antibody (Bio-Rad Laboratories). Chemiluminescent assay was used for detection (Pierce, Rockford, IL).

Ras infections. Cen3tel cells at different population doublings (PD) were infected with either the pWZL retroviral vector or its derivative with oncogenic *ras* (H-RasV12) as described previously (27). Infected cell populations were then selected in hygromycin (100 μg/mL) for 3 days.

Results

Tumorigenicity in nude mice. As described previously, cen3 primary fibroblasts were infected with an *hTERT*-containing

Table 1. Percentage of hyperdiploid mitoses in cen3tel cells at different PDs in culture

Cell line	Cen3	Cen3tel									
PD	16	18	44	63	76	108	118	124	130	139	165
% Hyperdiploid mitoses	2.6	1.5	1.2	4.2	4.2	10.7	12.9	35.9	42.6	65	100

retrovirus at PD 17 and were then propagated in culture. The infected population, named cen3tel, was telomerase positive and bypassed senescence (25). The ability of cen3tel cells to form tumors in nude mice was tested after 17 PDs since infection with the *hTERT* retrovirus (at PD 34) and at PD 107, when cells had already acquired the ability to grow in the absence of solid support). Cells at both passages did not form tumors even after 3 months since inoculation into the mice (25).

We have then inoculated cen3tel cells at PD 153 in nude mice and found that four of the five injected mice developed a tumor within 1 month since inoculation. One tumor was explanted and fragments of it were inoculated into three mice; two of them developed a tumor within 20 days. Thus, we can conclude that cen3tel cells became neoplastically transformed during culture propagation. A decrease in the latency of the tumors was observed when cells at PD 617 were inoculated in nude mice; in fact, after only 8 days since inoculation, six of six mice developed a tumor.

Karyotype and centrosome analysis. Besides the trisomies for three specific chromosomes and the structural chromosomal anomalies detected in cen3tel cells after PD 45 (25), we have observed a transition toward a heteroploid condition during culture propagation. As shown in Table 1, the frequency of hyperdiploid mitoses gradually increased with PD number. In cen3tel cells up to PD 76, the percentage of hyperdiploid mitoses ranged between 1.2% and 4.2% and then gradually increased up to 65% at PD 139 and subsequently reached 100% at PD 165. In these cells, the number of chromosomes ranged from 52 to 97; 60% of the mitoses contained between 75 and 80 chromosomes.

Because in tumor cells aneuploidy is frequently associated with amplification of centrosomes, the cytoplasmic organelles deputed to the formation of bipolar mitotic spindles (28), we analyzed the centrosome number in cen3 parental fibroblasts and in cen3tel cells at PDs 31, 81, 181, and 197. Centrosomes were stained by indirect immunofluorescence with a monoclonal antibody against γ-tubulin and their number was counted. In primary cen3 cells, the percentage of nuclei with more than two signals (three or four) was 2.4, and similar values were found in all the cen3tel samples at different PDs (from 0.0% in cen3tel PD 81 to 2.9% in cen3tel PD 197). Thus, aneuploidy was not paralleled by an increase in centrosome number or by spindle anomalies as assessed by indirect immunofluorescence staining of mitotic cells with an antibody against the spindle protein α-tubulin (Supplementary Fig. S1).

Contact growth inhibition, serum dependence, and morphologic changes. Normal fibroblasts in culture are characterized by contact inhibition (i.e., cells stop dividing when they form a monolayer and touch each other); in contrast, a characteristic of transformed cells is the capability to keep on dividing despite a high cell density and to pile up. To test whether cen3tel cells retained contact inhibition, we evaluated the percentage of S-phase cells in cultures at low and high cellular density. Primary cen3 fibroblasts and cen3tel cells at different PDs were seeded at low density and were incubated with bromodeoxyuridine for 30 minutes either 1 or 6 days after seeding. As shown in Table 2, a high percentage of cells incorporating bromodeoxyuridine was present in all the cell lines 1 day after seeding, indicating that cells were actively dividing; 6 days later, the percentage of S-phase cells was drastically reduced in cen3 primary cells and cen3tel cells between passages 24 and 28 while remained almost unchanged in cen3tel cells at later passages.

When maintained for 6 days in low serum concentration, cen3 primary fibroblasts and early PD cen3tel cells did not reach confluence and showed a greater reduction in the proportion of cells in S phase compared with the cells maintained in 10% serum (Table 2), indicating that both these cell lines require serum to grow. In cen3tel cells between PDs 114 and 120, the percentage of cells incorporating bromodeoxyuridine was reduced to 50% compared with cells grown in 10% serum, whereas in cen3tel cells at later PDs (between PDs 146 and 206) it remained unchanged. This result shows a progressive decline in the requirement of exogenous growth factors during transformation.

Cen3tel cells at different stages of culture propagation were also characterized by different morphologies. In Fig. 1, pictures of cells grown for 8 days are shown. Young cen3tel cells showed morphology similar to that of primary cen3 fibroblasts (Fig. 1*A* and *B*); cen3tel cells at mid passages (PD 98) retained an elongated fibroblastic morphology but reached a greater cellular density (Fig. 1*C*). Cen3tel cells at later passages (PDs 163 and 254) were characterized by a polygonal shape (Fig. 1*D* and *E*).

***INK4A* and c-*myc* expression.** We first analyzed the expression of the *INK4A* locus in cen3tel cells at different stages of propagation by Northern blot using the entire $p16^{INK4A}$ cDNA as a probe. As shown in Fig. 2*A*, we found similar levels of *INK4A* RNA in primary cen3 cells (Fig. 2*A, lane 1*) and in cen3tel cells at early passages (Fig. 2*A, lane 2*), whereas *INK4A* expression was

Table 2. Contact growth inhibition and serum dependence in cen3tel cells

Cell line	% ± SD of S-phase cells		
	10% serum		0.5% serum
	1 d	6 d	6 d
Primary cen3 (PD 17-20)	27.5 ± 9.9	6.6 ± 3.9	3.1 ± 3.4
Early cen3tel (PD 24-28)	36.4 ± 2.5	6.5 ± 2.7	2.4 ± 1.7
Mid cen3tel (PD 114-120)	41.8 ± 6.3	35.5 ± 7.1	14.4 ± 2.3
Late cen3tel (PD 146-209)	36.8 ± 6.3	36.6 ± 7.1	33.1 ± 3.7

NOTE: In cen3tel cells at different PDs, the percentage of S-phase cells was evaluated in proliferating cells (1 day after seeding), in confluent cell cultures (6 days after seeding), and in cultures grown for 6 days in low serum concentration.

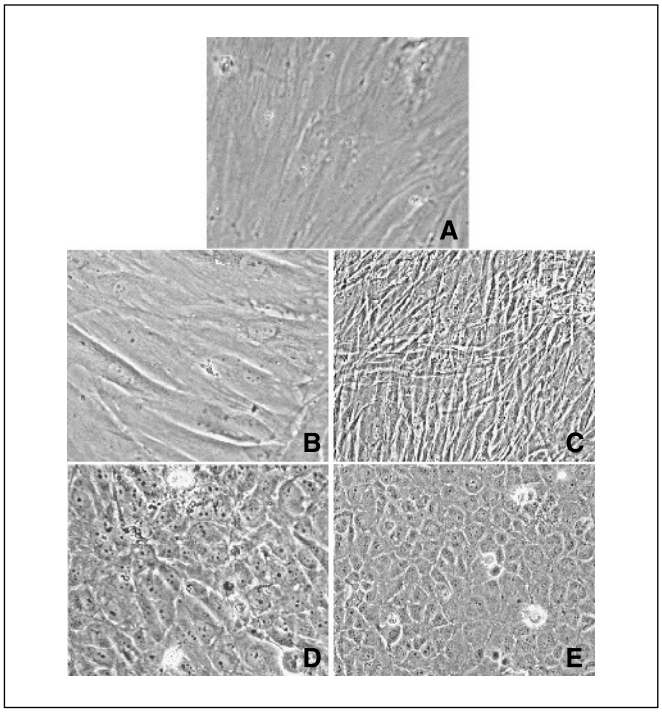

Figure 1. Morphology of cen3 primary fibroblasts at PD 21 (*A*) and cen3tel cells at different PDs: early cen3tel cells (PD 29; *B*), mid-passage cen3tel cells (PD 98; *C*), and late cen3tel cells (PDs 163 and 254; *D* and *E,* respectively). Taken at ×10 objective.

down-regulated in cen3tel cells at passage 108 (Fig. 2*A, lane 3*) and not detectable in cells at later passages (Fig. 2*A, lanes 4* and *5*). To examine the expression of the single $p16^{INK4A}$ and $p14^{ARF}$ genes, we did RT-PCR with primers specific for each gene (Fig. 2*B*), and we found that the expression of both genes was down-regulated in mid-passage cen3tel cells (Fig. 2*B, lane 3*) and untraceable in late cen3tel cells (Fig. 2*B, lanes 4* and *5*). At the protein level, $p16^{INK4}$ was undetectable also in cen3tel cells at mid passages (Fig. 2*C, lane 3*), despite the presence of RNA transcripts, as well as in late cen3tel cells (Fig. 2*C, lanes 4-6*).

In contrast, the c-*myc* oncogene, while expressed at similar levels in primary cen3 fibroblasts (Fig. 2*D, lane 1*) and cen3tel cells at early and mid passages (Fig. 2*D, lanes 2* and *3*), was clearly induced in cells at late passages (Fig. 2*D, lanes 4* and *5*). The increased c-*myc* mRNA level was paralleled by increased levels of the c-Myc protein (Fig. 2*E, lanes 4-6*).

***p53* and $p21^{CIP1}$ expression.** To test whether *p53* underwent mutation during cen3tel propagation, we first did a functional assay. We analyzed p53 cellular localization and nuclear accumulation after DNA damage by indirect immunofluorescence. Functional p53 is barely detectable in untreated cells, whereas it accumulates in the nucleus after DNA damage (29). In contrast, when large amounts of p53 can be detected in untreated cells, it is likely that the protein is stabilized by a mutation (30). As shown in Fig. 3, in primary cen3 fibroblasts as well as in early and mid PD cen3tel cells, p53 was clearly detected only after UV irradiation (Fig. 3*A-L*); in contrast, in cen3tel cells at PD 132, large amounts of nuclear p53 were observed in both untreated and UV irradiated cells (Fig. 3*M-P*), suggesting the presence of a p53 mutated form. By Western blot analysis, we observed that accumulation of p53 in cen3tel cells at late PDs (Fig. 4*A, lanes 4-6*) was paralleled by a decrease in the basal level of $p21^{CIP1}$ (Fig. 4*B, lanes 4-6*).

To confirm that *p53* underwent mutation during cen3tel culture propagation, we cloned the full-length *p53* cDNA prepared from primary cen3 cells and cen3tel cells at PDs 33, 46, 108, 165, and 366 and sequenced five cDNA clones for each cDNA. All the clones from primary fibroblasts and cen3tel cells up to passage 108 had the same wild-type sequence. All the clones from cen3tel cells at late passages (PDs 165 and 366) had a mutation in codon 161, which led to the substitution of an alanine with a threonine (GCC>ACC). The base substitution in the mutated allele causes the loss of a *Nco*I restriction enzyme target site. We found that the *p53* cDNA obtained from both late cen3tel cell samples was resistant to *Nco*I digestion (data not shown); this indicates that the mutated form is the only p53 form present in these cells probably due to loss of the second allele.

Mutational analysis of the *ras* genes and infection with activated Ras. Because activation of the H-*ras*, K-*ras*, and N-*ras* proto-oncogenes by point mutations in codon 12, 13, or 61 is a frequent genetic alteration associated with human cancers (31), we sequenced the regions of the *ras* genes containing the mutation hotspots in cen3tel cells at PD 153, when we found tumor

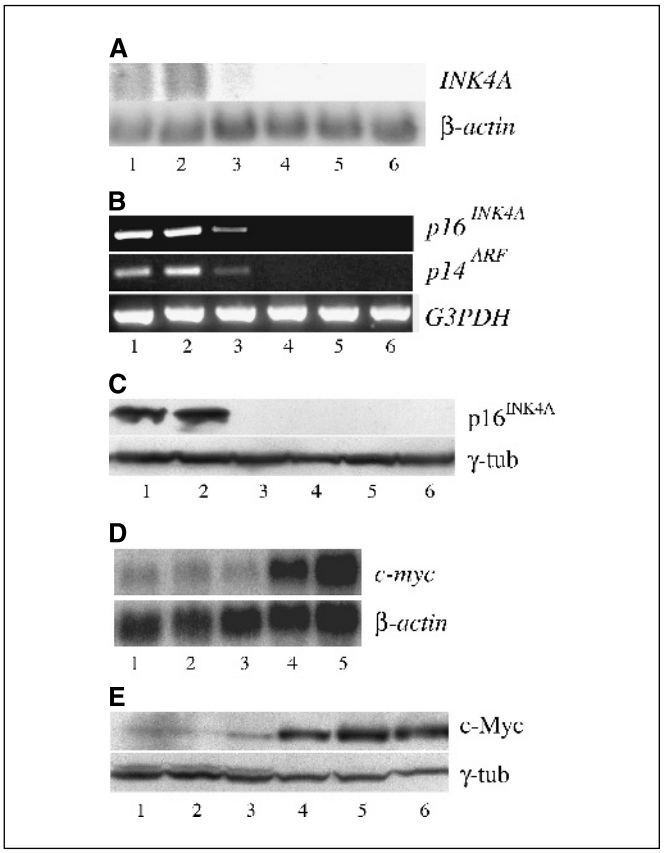

Figure 2. Analysis of the expression of *INK4A* and c-*myc* in cen3 and cen3tel cells at different PDs. *A* and *D,* Northern blotting using as probes the $p16^{INK4A}$ cDNA (*A*) and part of the third exon of the c-*myc* oncogene (*D*). *Lane 1,* primary cen3 fibroblasts (PD 22); *lane 2,* cen3tel (PD 46); *lane 3,* cen3tel (PD 108); *lane 4,* cen3tel (PD 171); *lane 5,* cen3tel (PD 366); *lane 6,* KATO III cells. KATO III RNA was used as negative control for *INK4A* expression (47). Hybridization with the probe for β-actin was performed as RNA loading control. *B,* RT-PCR with primers specific for $p16^{INK4A}$, $p14^{ARF}$, and *GAPDH* cDNAs. *Lane 1,* primary cen3 fibroblasts (PD 22); *lane 2,* cen3tel (PD 46); *lane 3,* cen3tel (PD 108); *lane 4,* cen3tel (PD 165); *lane 5,* cen3tel (PD 366); *lane 6,* KATO III cells. *C* and *E,* Western blot analysis of $p16^{INK4A}$ (*C*) and c-Myc (*E*). *Lane 1,* cen3 fibroblasts (PD 19); *lane 2,* cen3tel (PD 39); *lane 3,* cen3tel (PD 99); *lane 4,* cen3tel (PD 168); *lane 5,* cen3tel (PD 311); *lane 6,* cen3tel (PD 513). γ-Tubulin (*γ-tub*) was used as control for protein loading.

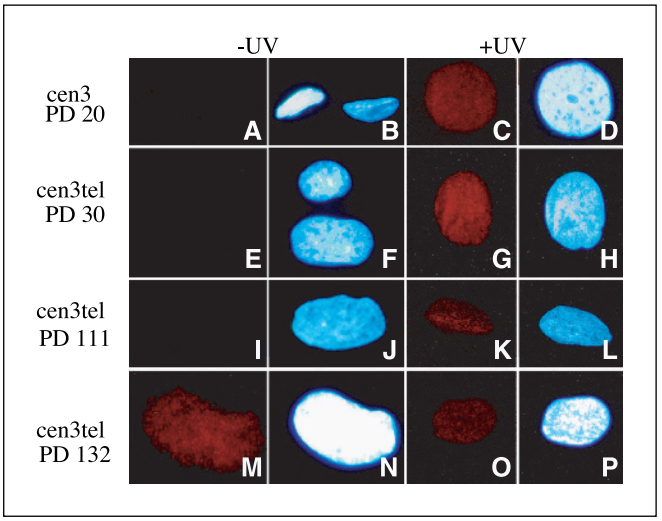

Figure 3. Indirect immunofluorescence detection of p53 in cen3 primary fibroblasts and cen3tel cells at different PDs. *A* to *D,* cen3 primary fibroblasts (PD 20); *E* to *H,* cen3tel (PD 30); *I* to *L,* cen3tel (PD 111); *M* to *P,* cen3tel (PD 132). *A, B, E, F, I, J, M*, and *N,* unirradiated cells; *C, D, G, H, K, L, O*, and *P,* UV irradiated cells (20 J/m^2). *A, E, I, M, C, G, K*, and *O,* indirect immunofluorescence with an anti-p53 monoclonal antibody; *B, F, J, N, D, H, L*, and *P,* the same cells in the indirect immunofluorescence analysis counterstained with 4′,6-diamidino-2-phenylindole.

induction for the first time, in cen3tel cells at PD 575 and in two tumor cell lines, one derived from cen3tel cells at PD 153 and the other from cen3tel cells at PD 617. In cen3tel cells at both passages and in the tumor cell line derived from cells at PD 617, we did not find mutations in the *ras* genes; in contrast, in the tumor cell line derived from cen3tel cells at passage 153, there was a mutation in K-*ras* codon 12 (GGT>GCT) in heterozygote condition. We also checked cen3tel cells for mutations in the exons 11 and 15 of the B-*raf* gene (32), which is a downstream effector of *ras*, and we did not find mutations in cen3tel cells at both PDs.

Infection with an activated *ras* induces a senescence growth arrest in primary cells (27). This form of senescence, similarly to replicative senescence, is considered a mechanism of cellular defense against oncogenic stimuli. Primary cen3 fibroblasts and cen3tel cells at passages 33, 105, and 170 were infected with a retrovirus carrying an activated *ras* oncogene or with an empty retrovirus as a control. In *ras*-infected cen3 fibroblasts and early cen3tel cells, we observed growth arrest and the acquisition of a typical senescent morphology (Fig. 5*B* and *D* compared with control cells in Fig. 5*A* and *C*). In the cells at these stage of propagation, 100% of the *ras*-infected cells showed staining for senescence-associated β-galactosidase. Mid and late cen3tel populations infected with *ras* did not show morphologic changes (Fig. 5*E* and *G* versus Fig. 5*F* and *H*). About 30% of cen3tel cells at PD 105 and 12% of cen3tel cells at PD 170 were positive to β-galactosidase. Thus, we can conclude that mid and late PD cen3tel cells can overcome the Ras-induced arrest and bypass the senescence checkpoint.

Conclusions and Discussion

Cen3 primary fibroblasts transduced with an *hTERT*-containing retrovirus gave rise to a telomerase-expressing immortal population, cen3tel, which gradually acquired a neoplastic phenotype during culture propagation.

Different results have been obtained by other authors when human somatic cells were immortalized through ectopic telomerase expression. Although several reports showed that telomerase immortalized cells maintained a normal phenotype without the development of cancer-associated features (24), recent data have shown that immortalization can be associated with the development of a preneoplastic or neoplastic phenotype. A common observation in these immortal telomerase-expressing cells was the loss of expression of the $p16^{INK4A}$ tumor suppressor gene (33–37). Overexpression of c-*myc* was also detected (34, 38), and in one cell line, *p53* underwent mutation (36). Among these cell lines, only those derived from mesenchymal stem cells induced tumor formation in nude mice (33).

To our knowledge, cen3tel is the first fibroblast cell line immortalized with *hTERT*, which underwent neoplastic transformation. The availability of cen3tel cells at different stages of their life span gave us the opportunity to trace specific changes associated with the acquisition of the transformed phenotype. We identified three major phases in the life span of cen3tel cells, each of which showed specific molecular and cytologic characteristics (Table 3).

During the first part of their life span (for ~60 PDs), early cen3tel cells maintained a morphology and a behavior similar to that of parental fibroblasts: they showed a typical fibroblastic morphology and contact inhibition and did not grow either in low serum concentration or in the absence of solid support; moreover, they retained the expression of $p16^{INK4A}$ and $p14^{ARF}$, normal levels of c-*myc* RNA, and wild-type *p53*.

During propagation, cen3tel cells, gradually increased their growth rate compared with normal cen3 fibroblasts (25). Cen3tel cells at mid passages (PD ~100) still retained a fibroblastic morphology but did not display contact inhibition anymore; they proliferated at low serum concentration, although the percentage of S-phase cells was lower than in complete medium, and showed the ability to grow in semisolid medium. The acquisition of these features, which are characteristic of transformed cells, was paralleled by a down-regulation of $p16^{INK4A}$ and $p14^{ARF}$ expression. A growth advantage in human cells in which $p14^{ARF}$ and $p16^{INK4A}$ had been knocked down by RNA interference was also described by Voorhoeve and Agami (23). In contrast to our results, other authors reported that $p16^{INK4A}$-deficient cells, or cells deficient in both $p16^{INK4A}$ and $p14^{ARF}$, do not display any ability to grow in the absence of solid support (23, 34, 39). This divergence could be due to differences in the cellular systems and/or to the presence in cen3tel cells of additional mutations thus far unknown, which cooperate with *INK4A* deficiency in allowing anchorage-independent growth. We can reasonably exclude that mutations in the *p53* gene are required for the growth in the absence of solid support, because cen3tel cells at

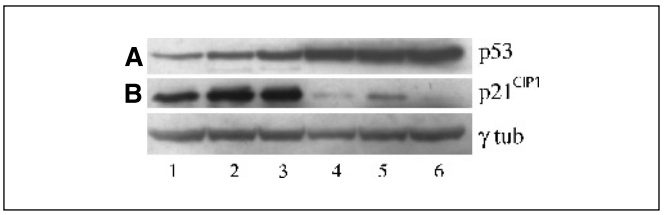

Figure 4. Western blot analysis of p53 (*A*) and $p21^{CIP1}$ (*B*) in cen3 primary fibroblasts and cen3tel cells at different PDs. *Lane 1,* cen3 fibroblasts (PD 19); *lane 2,* cen3tel (PD 39); *lane 3,* cen3tel (PD 99); *lane 4,* cen3tel (PD 168); *lane 5,* cen3tel (PD 311); *lane 6,* cen3tel (PD 513). γ-Tubulin was used as control for protein loading.

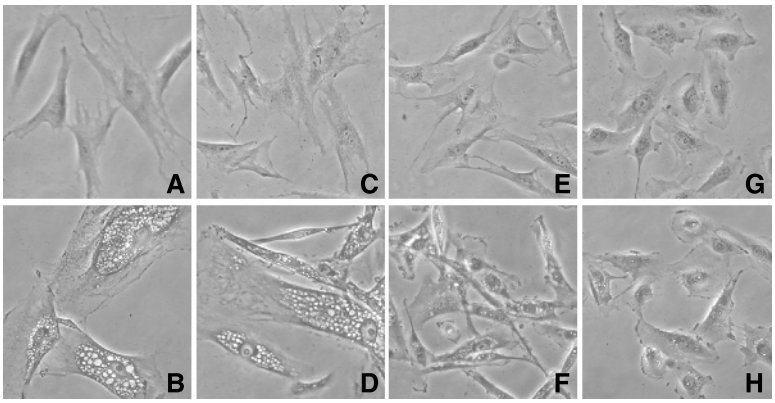

Figure 5. Infection of cen3 primary fibroblasts and cen3tel cells at different PDs with a retrovirus carrying an activated *ras*. *A*, *C*, *E*, and *G*, cells infected with an empty retrovirus; *B*, *D*, *F*, and *H*, cells infected with oncogenic *ras*. *A* and *B*, primary cen3 fibroblasts (PD 22); *C* and *D*, early cen3tel cells (PD 33); *E* and *F*, mid-passage cen3tel cells (PD 105); *G* and *H*, late cen3tel cells (PD 173).

mid passages still have a wild-type *p53* gene and a normal p53 response to UV irradiation.

At this stage of propagation, cen3tel cells were not tumorigenic in nude mice, indicating that *INK4A* deficiency per se is not sufficient for the development of a neoplastic phenotype. In contrast, mid-passage cen3tel cells showed a greater tolerance to Ras-induced senescence, suggesting that *INK4A* deficiency, without any apparent p53 impairment, allows cells to counteract induction of the senescence pathway by Ras. In human cells, contrasting results have been presented on the effect of the abrogation of the p16/pRB pathway on Ras-induced cellular senescence. The use of an excess of cdk4, a mutant form of this kinase insensitive to $p16^{INK4A}$, or small interfering RNA against $p16^{INK4A}$ RNA did not prevent Ras-induced growth arrest (23, 40). In contrast, mutations in $p16^{INK4A}$ directly abolishing the expression of the gene made a human fibroblast cell line resistant to Ras-induced senescence (41). Recently, Beausejour et al. (42) showed that transformation of human fibroblasts by oncogenic Ras is independent of *p53* and $p21^{CIP1}$ but requires complete or partial inactivation of the *INK4A* locus. The different results reported above could depend on the degree of inhibition of $p16^{INK4A}$ expression (39). In cen3tel at mid passages, the low residual level of $p16^{INK4A}$ can account for its resistance to Ras-induced senescence.

Two major genetic changes were observed in cen3tel cells at later passages: the loss of function of p53 and the increased expression of the c-*myc* oncogene. An alteration in p53 functionality was suggested by the observation that the protein accumulated in the nucleus of late cen3tel cells independently of a stressful treatment and was confirmed by sequence analysis of the *p53* cDNA, which revealed a mutation in the DNA-binding region at codon 161. Because the mutated cDNA was the only one detected in late cen3tel cells, loss of heterozygosity should have occurred during cen3tel propagation. The G>A transition present in codon 161 (GCC/ACC) leads to the substitution of an alanine with a threonine. Mutations at codon 161 have been found in several tumors, mainly solid tumors, and in about half of them, the same transition observed in cen3tel cells was present (see the IARC TP53 database at the Web site: http://www.iarc.fr/p53/). In parallel to the loss of p53 function, we observed a down-regulation of $p21^{CIP1}$.

Cen3tel cells at late passages did not show a classic fibroblastic morphology but were smaller and showed a polygonal shape typical of transformed cells, which suggests a change in cytoskeleton

Table 3. Summary of cellular and genetic characteristics of cen3tel cells at different stages of transformation

	Culture stage			
	Primary cen3 fibroblasts	Early cen3tel (<75 PDs)	Mid cen3tel (76*-130 PDs)	Late cen3tel (>130 PDs)
% Hyperdiploid mitoses	2.6	1.5-4.2	65	100
Contact growth inhibition	+	+	−	−
Serum dependence	+	+	+/−	−
Growth in agar	−	−	+	+
$p16^{INK4A}$ expression	+	+	+/−	−
$p14^{ARF}$ expression	+	+	+/−	−
Ras-induced growth arrest	+	+	+/−	−
p53 mutation	−	−	−	+
p21 expression	+	+	+	+/−
c-*myc* overexpression	−	−	−	+
Tumorigenicity	ND	−	−	+

NOTE: ND, not determined.
*At PD 76, we first detected anchorage-independent growth in cen3tel cells (25).

organization. In addition, they grew well in low serum concentration, indicating that they are able to produce autocrine growth factors; autocrine production of growth factors was seen in $p16^{INK4A}$-deficient fibroblasts transformed with c-*myc* oncogene (39). Cen3tel cells carrying the *p53* mutation and overexpressing c-*myc* were tumorigenic in nude mice.

Recently, several groups have succeeded in the malignant transformation of primary human cells using defined genetic elements, which lead to the perturbation of specific signaling pathways (39, 43). Although dysregulation of the Ras pathway by transfection with an activated H-*ras* gene was a common requirement to achieve transformation in the different protocols, we did not find activating mutations in H-*ras*, N-*ras*, and K-*ras*, or in their downstream effector B-*raf*, in cen3tel cells at any stage of propagation. We found a mutation in K-*ras* codon 12 in a cell line derived from a tumor developed by a mouse inoculated with cen3tel cells at passage 153 but not in tumor cells derived from a mouse inoculated with cells at passage 617. The presence of the mutation in one tumor cell line only indicates that it occurred during the growth of the tumor and suggests that, in tumorigenic cells, the Ras pathway was not already activated through a different route. Thus, our results suggest that spontaneous transformation of human immortalized fibroblasts does not require dysregulation of the Ras pathway.

To our knowledge, human fibroblast transformation protocols based on inactivation of $p16^{INK4A}$, $p14^{ARF}$, and *p53* and overexpression of c-*myc* (i.e., on the genetic alterations found in tumorigenic cen3tel cells) have not been tested yet. It has been shown that c-Myc cooperates with activated Ras in rendering tumorigenic $p16^{INK4A}$-deficient fibroblasts, but it is not sufficient to make these cells tumorigenic (44). Because in the c-Myc-transformed cells p53 was still functional, it is possible that a cooperation between c-Myc activation and p53 deficiency is required to get transformation.

Cen3tel cells are characterized by chromosomal instability (25). As shown previously (25), in cen3tel cells at early passages, trisomies for three specific chromosomes (7, 14, and 21) and sporadic structural rearrangements were present. Subsequently, at mid passages, the majority of the metaphases displayed clonal chromosomal rearrangements (25), and an increasing percentage of hyperdiploid mitoses was observed (Table 1); however, the clonal chromosomal anomalies were not related either to the ability to grow in agar or to transformation. At later passages, when cen3tel cells were tumorigenic, almost all the cells were subtetraploid (Table 1) as well as the cells derived from the tumors themselves (data not shown). However, despite the transition toward a heteroploid condition, we did not detect centrosome aberrations at any stage of propagation; thus, the aberrant chromosome number does not seem to depend on a variation in the centrosome number. It is likely that the numerical chromosomal variations, initially observed for a few specific chromosomes, reflect the instability already present in primary cen3 fibroblasts (25, 45); however, this instability was not sufficient per se to induce transformation of the primary cell. Evidence has been reported that aneuploid genomes are intrinsically unstable (46), being more prone to undergo further chromosome rearrangements and epigenetic modifications than normal cells; thus, the initial instability may have predisposed cen3tel cells to the development of an aberrant karyotype, which might have in turn facilitated neoplastic transformation.

Cen3tel is the first fibroblast cell line immortalized with *hTERT* in which successive steps could be identified during transformation at both molecular and cytologic levels (Table 3). In particular, we could define an initial phase of transformation, in which the cells were able to grow in the absence of solid support, displayed a down-regulation of the *INK4A* locus, but were not tumorigenic *in vivo*, and a successive phase, in which cells acquired *p53* mutations, overexpressed c-*myc*, and became able to form tumors in immunocompromised mice. Thus, our data indicate that besides stem cells (33), differentiated cells, such as fibroblasts, also can be targets for neoplastic transformation. In addition, karyotype instability seems to be a peculiar feature of cen3tel cells, because in most *hTERT* immortalized cell lines the karyotype remained essentially stable.

In conclusion, the results presented here support the view of cellular senescence as a tumor suppressor mechanism; in fact, they show that the abrogation of cellular senescence by ectopic telomerase expression can be associated with the gradual accumulation of mutations leading to the development of a neoplastic phenotype. In addition, our results allowed us to associate a down-regulation of the *INK4A* locus with anchorage-independent growth and with resistance to *ras*-induced senescence and to relate *p53* mutations and c-*myc* overexpression with tumorigenicity in nude mice.

Acknowledgments

Received 4/4/2005; revised 7/20/2005; accepted 10/12/2005.

Grant support: European Union grant FIGHT-CT 2002-217 and Italian Ministero dell'Istruzione dell'Università e della Ricerca grants FIRB RBNE01RNN7 and RBAU01ZB78 (C. Mondello) and European Union grant LSHC-CT-2004-502943 (M. D'Incalci).

The costs of publication of this article were defrayed in part by the payment of page charges. This article must therefore be hereby marked *advertisement* in accordance with 18 U.S.C. Section 1734 solely to indicate this fact.

We thank A. Ivana Scovassi, Ilaria Chiodi, and Roberta Guglielmino (Istituto di Genetica Molecolare-Consiglio Nazionale delle Ricerche) for their helpful advice, Fiorella Nuzzo for critical reading of the article, and G. Nadia Ranzani and Valentina Casazza (University of Pavia) for denaturing gradient gel electrophoresis analysis of the B-*raf* gene.

References

1. Blagosklonny MV. Cell immortality and hallmarks of cancer. Cell Cycle 2003;2:296–9.
2. Cech TR. Beginning to understand the end of the chromosome. Cell 2004;116:273–9.
3. de Lange T. Protection of mammalian telomeres. Oncogene 2002;21:532–40.
4. Greider CW, Blackburn EH. Tracking telomerase. Cell 2004;116:S83–6, 1 p. following S6.
5. Masutomi K, Yu EY, Khurts S, et al. Telomerase maintains telomere structure in normal human cells. Cell 2003;114:241–53.
6. Harley CB, Futcher AB, Greider CW. Telomeres shorten during ageing of human fibroblasts. Nature 1990;345:458–60.
7. Harley CB. Telomere loss: mitotic clock or genetic time bomb? Mutat Res 1991;256:271–82.
8. Bodnar AG, Ouellette M, Frolkis M, et al. Extension of life-span by introduction of telomerase into normal human cells. Science 1998;279:349–52.
9. de Lange T. Activation of telomerase in a human tumor. Proc Natl Acad Sci U S A 1994;91:2882–5.
10. d'Adda di Fagagna F, Reaper PM, Clay-Farrace L, et al. A DNA damage checkpoint response in telomere-initiated senescence. Nature 2003;426:194–8. Epub 2003 Nov 5.
11. Hara E, Tsurui H, Shinozaki A, Nakada S, Oda K. Cooperative effect of antisense-Rb and antisense-p53 oligomers on the extension of life span in human diploid fibroblasts, TIG1. Biochem Biophys Res Commun 1991;179:528–34.
12. Shay JW, Pereira-Smith OM, Wright WE. A role for both RB and p53 in the regulation of human cellular senescence. Exp Cell Res 1991;196:33–9.
13. Dimri GP, Campisi J. Molecular and cell biology of replicative senescence. Cold Spring Harb Symp Quant Biol 1994;59:67–73.
14. Ruas M, Peters G. The p16INK4a/CDKN2A tumor suppressor and its relatives. Biochim Biophys Acta 1998;1378:F115–77.
15. Alcorta DA, Xiong Y, Phelps D, Hannon G, Beach D,

Barrett JC. Involvement of the cyclin-dependent kinase inhibitor p16 (INK4a) in replicative senescence of normal human fibroblasts. Proc Natl Acad Sci U S A 1996;93:13742–7.
16. Collins CJ, Sedivy JM. Involvement of the INK4a/Arf gene locus in senescence. Aging Cell 2003;2:145–50.
17. Itahana K, Zou Y, Itahana Y, et al. Control of the replicative life span of human fibroblasts by p16 and the polycomb protein Bmi-1. Molecular and cell biology of replicative senescence. Mol Cell Biol 2003;23:389–401.
18. Herbig U, Jobling WA, Chen BP, Chen DJ, Sedivy JM. Telomere shortening triggers senescence of human cells through a pathway involving ATM, p53, and p21(CIP1), but not p16(INK4a). Mol Cell 2004;14:501–13.
19. Jacobs JJ, de Lange T. Significant role for p16(INK4a) in p53-independent telomere-directed senescence. Curr Biol 2004;14:2302–8.
20. Serrano M, Hannon GJ, Beach D. A new regulatory motif in cell-cycle control causing specific inhibition of cyclin D/CDK4. Nature 1993;366:704–7.
21. Krug U, Ganser A, Koeffler HP. Tumor suppressor genes in normal and malignant hematopoiesis. Oncogene 2002;21:3475–95.
22. Pomerantz J, Schreiber-Agus N, Liegeois NJ, et al. The Ink4a tumor suppressor gene product, p19Arf, interacts with MDM2 and neutralizes MDM2's inhibition of p53. Cell 1998;92:713–23.
23. Voorhoeve PM, Agami R. The tumor-suppressive functions of the human INK4A locus. Cancer Cell 2003; 4:311–9.
24. Harley CB. Telomerase is not an oncogene. Oncogene 2002;21:494–502.
25. Mondello C, Chiesa M, Rebuzzini P, et al. Karyotype instability and anchorage-independent growth in telomerase-immortalized fibroblasts from two centenarian individuals. Biochem Biophys Res Commun 2003;308: 914–21.
26. Mihic-Probst D, Perren A, Schmid S, Saremaslani P, Komminoth P, Heitz PU. Absence of BRAF gene mutations differentiates spitz nevi from malignant melanoma. Anticancer Res 2004;24:2415–8.
27. Serrano M, Lin AW, McCurrach ME, Beach D, Lowe SW. Oncogenic *ras* provokes premature cell senescence associated with accumulation of p53 and p16INK4a. Cell 1997;88:593–602.
28. Sluder G, Nordberg JJ. The good, the bad and the ugly: the practical consequences of centrosome amplification. Curr Opin Cell Biol 2004;16:49–54.
29. Lu X, Lane DP. Differential induction of transcriptionally active p53 following UV or ionizing radiation: defects in chromosome instability syndromes? Cell 1993; 75:765–78.
30. Moles JP, Moyret C, Guillot B, Jeanteur P, Guilhou JJ, Theillet C, Basset-Seguin N. p53 gene mutations in human epithelial skin cancers. Oncogene 1993;8:583–8.
31. Hingorani SR, Tuveson DA. Ras redux: rethinking how and where Ras acts. Curr Opin Genet Dev 2003; 13:6–13.
32. Mercer KE, Pritchard CA. Raf proteins and cancer: B-Raf is identified as a mutational target. Biochim Biophys Acta 2003;1653:25–40.
33. Serakinci N, Guldberg P, Burns JS, et al. Adult human mesenchymal stem cell as a target for neoplastic transformation. Oncogene 2004;23:5095–8.
34. Milyavsky M, Shats I, Erez N, et al. Prolonged culture of telomerase-immortalized human fibroblasts leads to a premalignant phenotype. Cancer Res 2003;63:7147–57.
35. Tsutsui T, Kumakura S, Yamamoto A, et al. Association of p16(INK4a) and pRb inactivation with immortalization of human cells. Carcinogenesis 2002;23:2111–7.
36. Noble JR, Zhong ZH, Neumann AA, Melki JR, Clark SJ, Reddel RR. Alterations in the p16(INK4a) and p53 tumor suppressor genes of hTERT-immortalized human fibroblasts. Oncogene 2004;23:3116–21.
37. Taylor LM, James A, Schuller CE, Brce J, Lock RB, Mackenzie KL. Inactivation of p16INK4a, with retention of pRB and p53/p21cip1 function, in human MRC5 fibroblasts that overcome a telomere-independent crisis during immortalization. J Biol Chem 2004;279:43634–45. Epub 2004 Aug 10.
38. Wang J, Hannon GJ, Beach DH. Risky immortalization by telomerase. Nature 2000;405:755–6.
39. Drayton S, Brookes S, Rowe J, Peters G. The significance of p16INK4a in cell defenses against transformation. Cell Cycle 2004;3:611–5. Epub 2004 May 9.
40. Wei W, Herbig U, Wei S, Dutriaux A, Sedivy JM. Loss of retinoblastoma but not p16 function allows bypass of replicative senescence in human fibroblasts. EMBO Rep 2003;4:1061–6. Epub 2003 Oct 17.
41. Brookes S, Rowe J, Ruas M, et al. INK4a-deficient human diploid fibroblasts are resistant to RAS-induced senescence. EMBO J 2002;21:2936–45.
42. Beausejour CM, Krtolica A, Galimi F, et al. Reversal of human cellular senescence: roles of the p53 and p16 pathways. EMBO J 2003;22:4212–22.
43. Boehm JS, Hahn WC. Understanding transformation: progress and gaps. Curr Opin Genet Dev 2005;15:13–7.
44. Drayton S, Rowe J, Jones R, et al. Tumor suppressor p16INK4a determines sensitivity of human cells to transformation by cooperating cellular oncogenes. Cancer Cell 2003;4:301–10.
45. Mondello C, Moralli D, Franceschi C, Nuzzo F. Occurrence and expansion of trisomy 7 in a fibroblast strain from a centenarian individual. Exp Gerontol 1999; 34:715–9.
46. Matzke MA, Mette MF, Kanno T, Matzke AJ. Does the intrinsic instability of aneuploid genomes have a causal role in cancer? Trends Genet 2003;19:253–6.
47. Iida S, Akiyama Y, Nakajima T, et al. Alterations and hypermethylation of the p14(ARF) gene in gastric cancer. Int J Cancer 2000;87:654–8.

Stepwise Neoplastic Transformation of a Telomerase Immortalized Fibroblast Cell Line

Samantha Zongaro, Elisa de Stanchina, Tina Colombo, et al.

Cancer Res 2005;65:11411-11418.